BMC Cancer

RESEARCH Open Access

Potential biomarkers develop for predicting the prognosis of patients with esophageal squamous cell carcinoma after optimized chemoradiotherapy using serum metabolomics

Jie Yang[1†], Yunyun Zhu[2†], Yijian Zhou[3,4], Jiaying Zhang[3,4], Yuxuan Wei[3,4], Yongpan Liu[5], Bo Zhang[3,4], Jialing Xie[3,4], Xiaolu An[3,4], Xianhua Qi[3,4], Yuting Yue[3,4], Lijia Zhang[3,4], Xiajun Zhang[1*], Zhichao Fu[2*] and Kuancan Liu[3,4*]

Abstract

Background Esophageal squamous cell carcinoma (ESCC), the most common type of esophageal cancer, characterized by low five-year survival rate, and concurrent chemoradiotherapy (CCRT) has been proposed to treat ESCC, while potential biomarkers for prognostic monitoring after optimized CCRT remains unknown.

Methods Serum samples from 45 patients with ESCC were collected and categorized into three groups: Control (pre-CCRT), CCRT (during CCRT), and CCRT-1 M (one-month post-CCRT). The therapeutic effect was evaluated using CT imaging and established evaluation criteria. Untargeted metabolomic analysis was performed on the serum samples to identify differential metabolites caused by CCRT treatment, assessing their potential for prognostic monitoring.

Results CCRT had significant therapeutic efficacy in patients with ESCC, as indicated by CT imaging and RECIST 1.1 solid tumor evaluation criteria. Notably, several metabolic markers were identified through non-targeted metabolomic analysis, highlighting changes following CCRT treatment. These differential metabolites are involved in the dysregulation of phenylalanine, tyrosine, and tryptophan biosynthesis, as well as histidine, arginine, and proline metabolism, and glycine, serine, and threonine metabolism, suggesting a reduction in glucose metabolism in patients with ESCC after CCRT. Additionally, ROC analysis indicated that the AUC of these metabolites exceeded 0.661, underscoring their diagnostic value for assessing CCRT efficacy and their potential use in prognostic monitoring.

†Jie Yang and Yunyun Zhu contributed equally to this work.

*Correspondence:
Xiajun Zhang
zxj477658333@sina.com
Zhichao Fu
fauster1112@126.com
Kuancan Liu
liukuancan@xmu.edu.cn

Full list of author information is available at the end of the article

Comparative metabolomic analysis identified L-phenylalanine and lysine as promising serum biomarkers for predicting therapeutic outcomes.

Conclusions CCRT shows considerable therapeutic benefit in patients with ESCC, with observed reductions in glucose metabolism post-treatment. L-phenylalanine and lysine may serve as potential serum biomarkers to predict CCRT efficacy.

Keywords Esophageal squamous cell carcinoma, Metabolomics, CCRT, Prognosis, Biomarkers

Background

Esophageal carcinoma, particularly esophageal squamous cell carcinoma (ESCC), ranks among the most prevalent malignant tumors in China, with surgical intervention recognized as the most effective treatment. Unfortunately, ESCC is often diagnosed only at intermediate or advanced stages, resulting in over half of patients being ineligible for curative surgery [1]. In clinical settings, concurrent chemoradiotherapy (CCRT) has emerged as a viable treatment option for patients who are unresectable or cannot tolerate surgical procedures, particularly for those in stage II or III [2]. Compared to surgical intervention alone, CCRT increases the resectability rate, diminishes the likelihood of postoperative recurrence and metastasis, and contributes to improved survival rates. Nonetheless, it has been reported that only 29% of patients undergoing CCRT achieve a complete pathological response [3], underscoring the significant variability in individual patient responses to treatment.

The development of ESCC is characterized as a multistage evolutionary process. To satisfy metabolic and energetic demands and adapt to microenvironmental changes during malignant transformation, the metabolic phenotype of tumor cells evolves, ultimately disrupting systemic metabolism [4], including alterations in amino acids, glucose, lipids, organic acids, nucleotides, and fatty acids [5]. Abnormal metabolites present in peripheral blood hold promise for cancer diagnosis, treatment efficacy evaluation, and prognostic prediction [6]. For instance, serum cross-linked carboxyterminal telopeptide of Type I collagen (ICTP) may be a novel prognostic marker for evaluating ESCC progression, as suggested by a study of 29 patients undergoing radical resection for ESCC [7].

However, the correlation between metabolite alterations in serum samples and the advancement of patients with esophageal cancer, as well as the outcome of CCRT treatment, remains ambiguous. Therefore, this study aims to optimize the therapeutic scheme for patients with ESCC utilizing CCRT and to identify potential biomarkers for monitoring prognosis.

Methods

Collection of clinical samples

Serum samples from 45 patients with stage II to IV esophageal cancer were prospectively collected at the 900 Hospital of the Joint Logistics Team (Dongfang Hospital, Xiamen University). The patients were divided into three groups: 17 patients prior to CCRT (Control group), 17 patients after completing CCRT (CCRT group), and 11 patients at one-month post-CCRT (CCRT-1 M group), all diagnosed with esophageal squamous cell carcinoma. The CCRT regimen consists of radiotherapy combined with concurrent chemotherapy, where chemotherapeutic agents are administered alongside radiation. The radical concurrent chemoradiotherapy consisted of 60 Gy, delivered in 30 fractions, with 5 fractions per week, and the concurrent chemotherapy regimens comprised as following: albumin paclitaxel 260 mg/m2 IV d1 along with nedaplatin 80 mg/m2 d1 or lobaplatin 40 mg/m2 d1, administered every 3 weeks. All enrolled patients underwent the same CCRT protocol, this treatment protocol enhances radiosensitization, improves local control, and reduces the risk of distant metastasis.

Therapeutic efficacy was evaluated using CT imaging, based on RECIST 1.1 criteria for solid tumors: a partial response (PR) is defined as a $\geq$ 30% reduction in the sum of diameters of all measurable target lesions relative to baseline, while stable disease (SD) indicates neither a sufficient reduction for PR nor an increase for progressive disease (PD). This study was carried out in accordance with the World Medical Association Declaration of Helsinki, and it was approved by the ethics committee of the 900 Hospital of the Joint Logistics Team (Dongfang Hospital, Xiamen University) (Approval No. 2022-049), clinical trial number: not applicable, and the informed consent were signed by patients involved in this study.

Serum collection

Blood samples were collected in centrifuge tubes at 37 °C (or room temperature) for one hour to allow coagulation. They were centrifuged at 3000 rpm for 10 min at room temperature, and the supernatant was transferred to clean tubes. The samples were then centrifuged again at 12,000 rpm for 10 min at 4 °C, with the resulting supernatant dispensed into 1.5 mL tubes at 0.2 mL per tube and stored at -80 °C.

Extraction of metabolites

For extraction, each sample was pipetted into EP tubes, and four volumes of extraction solution (methanol: acetonitrile = 1:1 (V/V)) containing an isotope-labeled internal standard were added. The mixture was vortexed for 30 s, sonicated for 10 min in an ice water bath, and then allowed to stand at -40 °C for one hour. Following centrifugation at 4 °C and 12,000 rpm for 15 min, the supernatant was collected for injection bottle testing. Equal volumes of supernatant from all samples were pooled to create quality control (QC) samples for further analysis.

LC-MS/MS analysis and data processing

For the analysis of polar metabolites, target compounds were separated on a Waters ACQUITY UPLC BEH Amide column (2.1 mm × 50 mm, 1.7 μm) using a Vanquish ultra-performance liquid chromatograph (Thermo Fisher Scientific). The mobile phase comprised an aqueous solution with 25 mmol/L ammonium acetate and 25 mmol/L ammonia (Phase A) and acetonitrile (Phase B). The sample tray was maintained at 4 °C, with an injection volume of 2 μL. Mass spectrometric data acquisition was performed using an Orbitrap Exploris 120, controlled by Xcalibur software (version 4.4, Thermo), enabling both primary and secondary mass spectrum data collection.

Key instrument parameters included: sheath gas flow rate at 50 Arb, auxiliary gas flow rate at 15 Arb, capillary temperature at 320 °C, full MS resolution at 60,000, MS/MS resolution at 15,000, collision energy set to stepped normalized collision energy (SNCE) levels of 20/30/40, and spray voltage at 3.8 kV (positive mode) or -3.4 kV (negative mode). Raw data were converted to mzXML format using ProteoWizard software, followed by metabolite identification using the R package and BiotreeDB (V3.0) as the database. Visualization analysis was subsequently performed using R.

Table 1 Details of clinical characteristics of patients

Sex	34 males
	11 females
Tumor location	8 cases in the middle and lower esophagus
	3 in the lower thoracic esophagus
	6 in the upper thoracic esophagus
	11 in the middle thoracic esophagus
	8 in the middle and upper esophagus
	5 in the upper cervical esophagus
	2 in the cervical and upper thoracic esophagus
	2 in the middle esophagus
Stage	17 cases at stage II
	25 cases at stage III
	3 cases at stage IV
Treatment response	43 cases PR
	2 cases SD

Statistical analysis

Paired t-test analysis are performed across Control, CCRT, and CCRT-1 M groups, and GraphPad PRISM V8.0 software was used for all analyses and repeated measures ANOVA was used to determine differences between groups. A P-value of less than 0.05 was deemed significant, * represents $P < 0.05$. ** represents $P < 0.01$, *** represents $P < 0.001$, and **** represents $P < 0.0001$.

Results

CCRT has a significant therapeutic effect on patients with ESCC

In this study, 45 serum specimens were collected from patients with ESCC, comprising 17 samples from the Control group, 17 from the CCRT group, and 11 from the CCRT-1 M group. Among these, there were 34 male and 11 female samples. Each patient received a pathological diagnosis confirming ESCC, with staging assessments indicating 17 cases at stage II, 25 at stage III, and 3 at stage IV. Tumor localization included 8 cases in the middle and lower esophagus, 3 in the lower thoracic esophagus, 6 in the upper thoracic esophagus, 11 in the middle thoracic esophagus, 8 in the middle and upper esophagus, 5 in the upper cervical esophagus, 2 in the cervical and upper thoracic esophagus, and 2 in the middle esophagus (Table 1).

Therapeutic efficacy was assessed using CT imaging in conjunction with RECIST 1.1 criteria for solid tumors. Of the 45 cases, 43 demonstrated PR, while 2 showed SD. Radiotherapy, alongside concurrent chemotherapy with paclitaxel and platinum-based agents, exhibited significant therapeutic efficacy in patients with ESCC. As depicted in Fig. 1, notable improvements were observed in three ESCC cases involving lower (Fig. 1A, B), upper (Fig. 1C, D), and middle (Fig. 1E, F) esophageal lesions before and after radical concurrent radiotherapy and chemotherapy. Additionally, post-treatment assessments revealed a reduction in metastatic lymph node size in the zone 1 esophageal region following radical chemoradiotherapy with a regimen of PGTV 60 Gy/30F/6 W and concurrent cisplatin plus fluorouracil (Fig. 1G, H). Thus, CCRT demonstrates a substantial therapeutic effect in patients with ESCC.

Differential metabolites were accompanied following CCRT treatment

Identifying a reliable biomarker for chemoradiotherapy sensitivity in ESCC is critical for optimizing patient prognosis and preventing delays in effective treatment. This study employed non-targeted metabolomic analysis, identifying 76 metabolites through NEG analysis and 103 metabolites through POS analysis. OPLS-DA plots revealed a clear separation in metabolic profiles across CCRT vs. Control, CCRT-1 M vs. Control, and

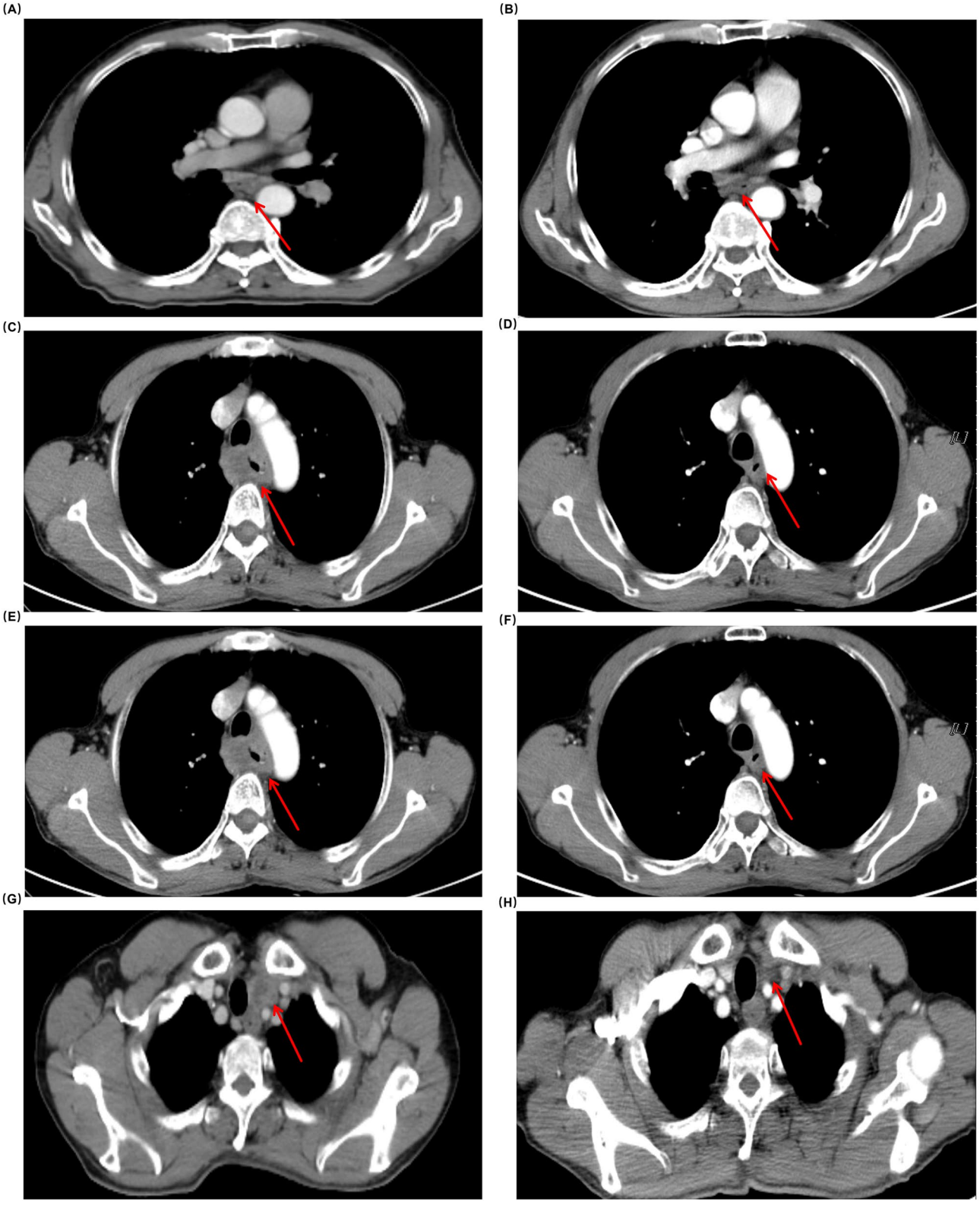

Fig. 1 (See legend on next page.)

(See figure on previous page.)

Fig. 1 Therapeutic impact of CCRT on patients with ESCC. **A** Lower esophageal carcinoma prior to radical chemoradiotherapy. **B** Post-treatment, the lower esophageal tumor shows significant reduction following a regimen of PGTV 60 Gy/30F/6 W and concurrent chemotherapy. **C** Upper esophageal carcinoma before radical concurrent chemoradiotherapy. **D** Post-treatment, upper esophageal carcinoma demonstrates a notable size reduction. **E** Middle esophageal carcinoma before radical chemoradiotherapy with PGTV 60 Gy/30F/6 W radiotherapy, in combination with paclitaxel and nedaplatin or lobaplatin chemotherapy. **F** Post-treatment, middle esophageal carcinoma is visibly reduced in size. **G** Metastatic lymph nodes in zone 1 of esophageal carcinoma prior to radical chemoradiotherapy. **H** Post-treatment, metastatic lymph nodes in zone 1 show a decrease in size under a PGTV 60 Gy/30F/6 W regimen with concurrent chemotherapy

CCRT-1 M vs. CCRT comparisons (Fig. 2), indicating distinct intergroup metabolic differences.

For the CCRT vs. Control comparison, NEG analysis identified 4 differential metabolites, and POS analysis identified 12, all showing down-regulated expression levels. In the CCRT-1 M vs. Control comparison, NEG analysis identified 15 differential metabolites (7 up-regulated, 8 down-regulated), while POS analysis identified 30 metabolites (9 up-regulated, 21 down-regulated). For the CCRT-1 M vs. CCRT comparison, NEG analysis detected 4 up-regulated differential metabolites, and POS analysis detected 2 differential metabolites, with 1 up-regulated and 1 down-regulated. Detailed results are available in Table 2; Fig. 3. Cluster analysis further demonstrated that up-regulated and down-regulated metabolites clustered distinctly, highlighting that these differential metabolites emerged in conjunction with CCRT treatment.

Glucose metabolism decreased in patients with ESCC following CCRT treatment

To further investigate the metabolic pathways associated with susceptibility to CCRT therapy in patients with ESCC, pathway analysis based on the KEGG database was conducted, with the findings presented in a rectangular tree diagram. In the CCRT vs. Control comparison, differential metabolites influenced pathways including phenylalanine, tyrosine, and tryptophan biosynthesis, phenylalanine metabolism, and arginine and proline metabolism (Fig. 4A, B). For the CCRT-1 M vs. CCRT comparison, affected pathways involved histidine metabolism, phenylalanine, tyrosine, and tryptophan biosynthesis, and tyrosine metabolism (Fig. 4C, D). In the CCRT-1 M vs. Control comparison, differential metabolites impacted phenylalanine, tyrosine, and tryptophan biosynthesis, as well as glycine, serine, and threonine metabolism, and tryptophan metabolism (Fig. 4E, F).

The pathway details include phenylalanine being oxidized to tyrosine by phenylalanine hydroxylase, both of which are involved in glucose and fat metabolism. Additionally, L-histidine is converted to glutamic acid *via* histidine enzyme, entering the tricarboxylic acid (TCA) cycle. Arginine, through the action of arginase, is broken down into ornithine and urea, contributing to the urea cycle, while proline, derived from glutamic acid, is ultimately converted to pyruvate for the TCA cycle. Glycine is transformed into pyruvate, which subsequently enters the gluconeogenic pathway to produce glucose; serine synthesis proceeds mainly through the L-serine branch pathway *via* 3-phosphoglycerate in glycolysis, with D-serine originating from L-serine racemization. Threonine undergoes conversion to glycine by aldolase.

These results highlight the dysregulation of metabolic pathways in patients with ESCC, particularly the biosynthesis of phenylalanine, tyrosine, and tryptophan, which appears closely linked to CCRT susceptibility. Alongside alterations in the expression of these amino acids, the results indicate that post-CCRT patients with ESCC exhibit reduced levels of glucose metabolism, encompassing glycolysis, the TCA cycle, and gluconeogenesis pathways.

Differential metabolites can be used to monitor or judge prognosis

ROC analysis was conducted to assess the potential of these differential metabolites as predictive markers for CCRT efficacy. In the NEG analysis, for the CCRT vs. Control comparison, the AUC values of 4 down-regulated metabolites ranged from 0.68 to 0.70. For CCRT-1 M vs. CCRT, the AUC of 4 up-regulated metabolites ranged from 0.74 to 0.86. For CCRT-1 M vs. Control, AUC values ranged from 0.69 to 0.99 for 7 up-regulated metabolites and from 0.78 to 0.91 for 8 down-regulated metabolites (Table 3).

In the POS analysis, for CCRT vs. Control, AUC values for 12 down-regulated metabolites ranged from 0.66 to 0.81. For CCRT-1 M vs. CCRT, AUC values for 2 metabolites ranged from 0.78 to 0.80. For CCRT-1 M vs. Control, AUC values for 9 up-regulated metabolites ranged from 0.72 to 0.88, and AUC values for 21 down-regulated metabolites ranged from 0.69 to 0.96 (Table 3). These results demonstrate that the AUC values of these metabolites consistently exceed 0.661, indicating their diagnostic value in evaluating CCRT efficacy and potential utility in prognostic monitoring.

L-phenylalanine and lysine may serve as potential serum biomarkers to predict the efficacy of CCRT

To identify serum metabolic markers that may predict CCRT efficacy, comparative metabolomic analyses were performed on 11 matched patients across Control, CCRT, and CCRT-1 M groups. Venn diagrams were used to illustrate the relationships among the differential metabolites in each comparison (Fig. 5). In the NEG analysis, comparisons between (CCRT vs. Control) and

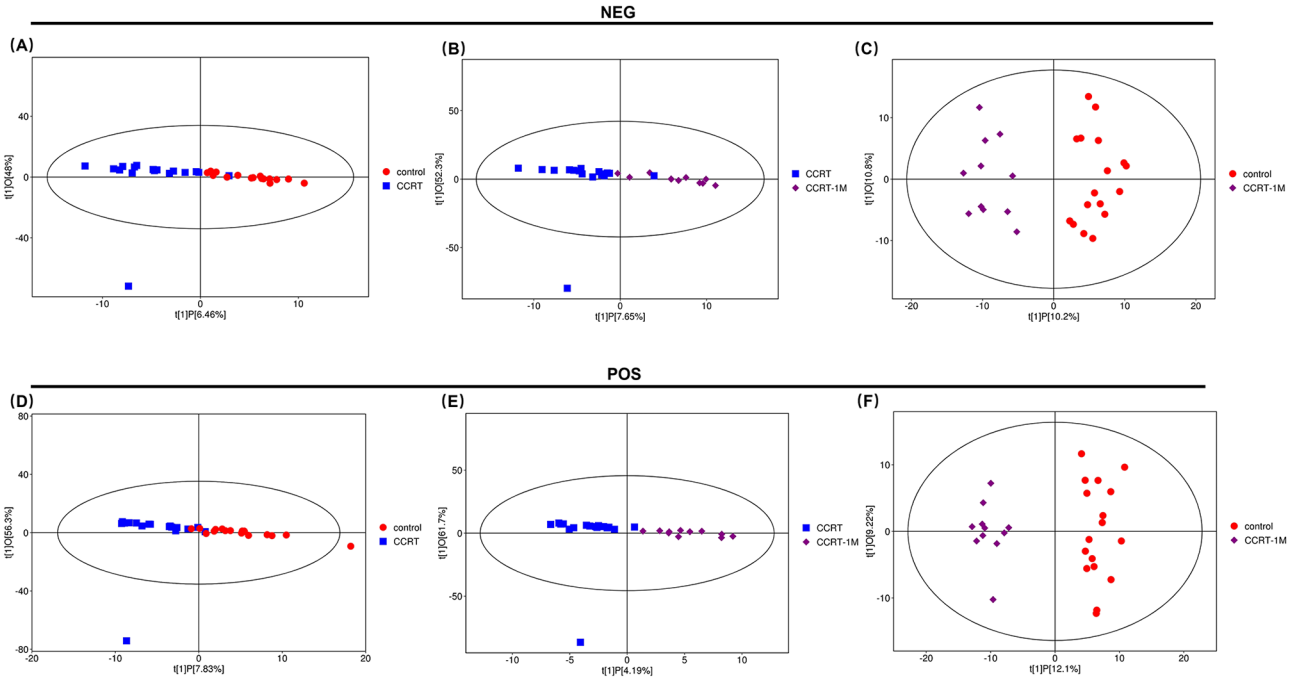

Fig. 2 OPLS-DA score scatter plots for metabolomic profiles of patients with ESCC. NEG Mode: **A** OPLS-DA score scatter plot for Control vs. CCRT group. **B** OPLS-DA score scatter plot for CCRT vs. CCRT-1 M group. **C** OPLS-DA score scatter plot for Control vs. CCRT-1 M group. POS Mode: **D** OPLS-DA score scatter plot for Control vs. CCRT group. **E** OPLS-DA score scatter plot for CCRT vs. CCRT-1 M group. **F** OPLS-DA score scatter plot for Control vs. CCRT-1 M group. In each plot, the horizontal axis (t [1]P) represents the predicted score of the first principal component, indicating intergroup variability, while the vertical axis (t [1]O) represents the orthogonal principal component score, showing intragroup consistency. Each scatter point symbolizes a sample, with its shape and color corresponding to different experimental groups. Greater horizontal distances indicate larger intergroup differences, while closer vertical proximity reflects better intragroup reproducibility. NEG: Negative ion mode; POS: Positive ion mode

(CCRT-1 M vs. Control) identified 3 metabolites—L-Phenylalanine, L-Threonine, and Xanthine—that continuously decreased with CCRT progression. Comparisons between (CCRT-1 M vs. Control) and (CCRT-1 M vs. CCRT) identified 2 metabolites, Neotrehalose and N-Acetyl-L-alanine, with Neotrehalose showing continuous up-regulation across the groups, while N-Acetyl-L-alanine exhibited an initial down-regulation followed by up-regulation.

In the POS analysis, comparisons between (CCRT vs. Control) and (CCRT-1 M vs. Control) revealed 10 differential metabolites ((+)-2,3-Dihydro-3-methyl-1 H-pyrrole, 2,6-diaminohexanoic acid (lysine), Pipecolic acid, L-Threonine, 1-Aminocyclopropanecarboxylic acid, Racemethionine, 2,4,6-Octatriynoic acid, Debrisoquine, Polyvidone, and LysoPC (18:3(6Z,9Z,12Z))), all of which displayed continuous down-regulation across the groups. Additionally, a differential metabolite, L-Tyrosine, identified in (CCRT-1 M vs. Control) and (CCRT-1 M vs. CCRT) comparisons, showed initial up-regulation followed by down-regulation.

Significant differences were observed for these differential metabolites across the three groups, as illustrated in Fig. 6. For CCRT vs. Control, the AUC for L-Phenylalanine was 0.682, and for Lysine, it was 0.810. In the CCRT-1 M vs. Control comparison, the AUC values were 0.904 for L-Phenylalanine and 0.947 for Lysine. Paired t-test analysis confirmed that L-phenylalanine and Lysine exhibited significant intergroup differences, suggesting that L-Phenylalanine and Lysine may serve as potential serum biomarkers to predict CCRT efficacy.

Discussion

The understanding of pathological mechanisms and factors involved in ESCC tumorigenesis is gradually advancing [8–10]. Current treatment options for ESCC include surgery, chemotherapy, radiotherapy, and neoadjuvant chemoradiotherapy. Beyond these conventional approaches, targeted therapy and immunotherapy have also emerged as promising strategies. Previous research established a peptide aptamer library and identified a peptide aptamer, P42, which targets the SOX2 protein. Both P42 and synthetic P42 were shown to attenuate the malignant behavior of ESCC cells in vitro and in vivo [11]. Additionally, PARP1 and CDP bind to SOX2, and targeting either PARP1 or CDP with 3-ABA or the peptide aptamer P58 inhibits various oncogenic processes in ESCC cells [12, 13]. Therapeutic efficacy was further validated on ESCC organoids using polysaccharides derived from Agaricus blazei murrill and Enteromorpha prolifera

Table 2 Distribution patterns of differential metabolites

CCRT vs. Control	NEG	down	L–Phenylalanine
			L–Threonine
			Uridine
			Xanthine
	OPS	down	2,6-diaminohexanoic acid
			Pipecolic acid
			Racemethionine
			Polyvidone
			L-Threonine
			(+)-2,3-Dihydro-3-methyl-1 H-pyrrole
			1-Aminocyclopropanecarboxylic acid
			L-Arginine
			2,4,6-Octatriynoic acid
			Cis-stilbene oxide
			LysoPC(18:3(6Z,9Z,12Z))
			Debrisoquine
CCRT vs. CCRT-1 M	NEG	up	1,5–Anhydrosorbitol
			L–Histidine
			N–Acetyl–L–alanine
			Neotrehalose
	POS	up	N-Methyl proline
		down	L-Tyrosine
CCRT-1 M vs. Control	NEG	up	10E,12Z–Octadecadienoic acid
			Acetylglycine
			Diethylphosphate
			Isovalerylglycine
			N–Acetyl–L–alanine
			N–Acetylserine
			Neotrehalose
		down	Hydroxyphenyllactic acid
			L–Methionine
			L–Norleucine
			L–Phenylalanine
			L–Proline
			L–Threonine
			L–Valine
			Xanthine
	OPS	up	N-nitrosomethanamine
			N, N-Dimethylformamide
			5′-Methylthioadenosine
			Phosphorylcholine
			2-(Ethylamino)-4,5-dihydroxybenzamide
			Hydroxyprolyl-Asparagine
			Acetic anhydride
			PC(18:2(9Z,12Z)/P-18:1(11Z))
			Lysyl-Isoleucine
		down	D-Proline
			L-Valine
			2,6-diaminohexanoic acid
			L-Glutamine
			Pipecolic acid
			Indoleacetaldehyde
			Ethyl carbamate
			Racemethionine
			Serotonin
			Polyvidone
			L-Threonine
			L-Tyrosine
			(+)-2,3-Dihydro-3-methyl-1 H-pyrrole
			1-Aminocyclopropanecarboxylic acid
			Methylnoradrenaline
			Piperidine
			2,4,6-Octatriynoic acid
			Glycine
			2-Benzofurancarboxaldehyde
			LysoPC(18:3(6Z,9Z,12Z))
			Debrisoquine

[14]. These results underscore the potential of discovering novel therapeutic targets or repurposing existing drugs to improve ESCC treatment outcomes.

Alongside treatment advancements, biomarkers for monitoring therapeutic progress and efficacy are also crucial in improving patient outcomes. Individual responses to CCRT vary significantly, and recent studies suggest that metabolic response assessment offers superior prognostic stratification over histopathological assessment in patients with esophageal adenocarcinoma undergoing neoadjuvant therapy [15]. Tyrosine, phenylalanine, and tryptophan have been proposed as potential biomarkers for gastroesophageal cancers, as a systematic review highlights their relevance in therapy for these malignancies. Six studies assessed serum concentrations of these aromatic amino acids, with all but one study reporting decreased levels; the exception observed an increase in phenylalanine [16]. These results align with our findings of dysregulated biosynthesis of phenylalanine, tyrosine, showing a continuous downregulation of phenylalanine with CCRT, a transient upregulation followed by downregulation of tyrosine, and an overall decline in their levels. These differential metabolites appear to be consistently associated with CCRT treatment.

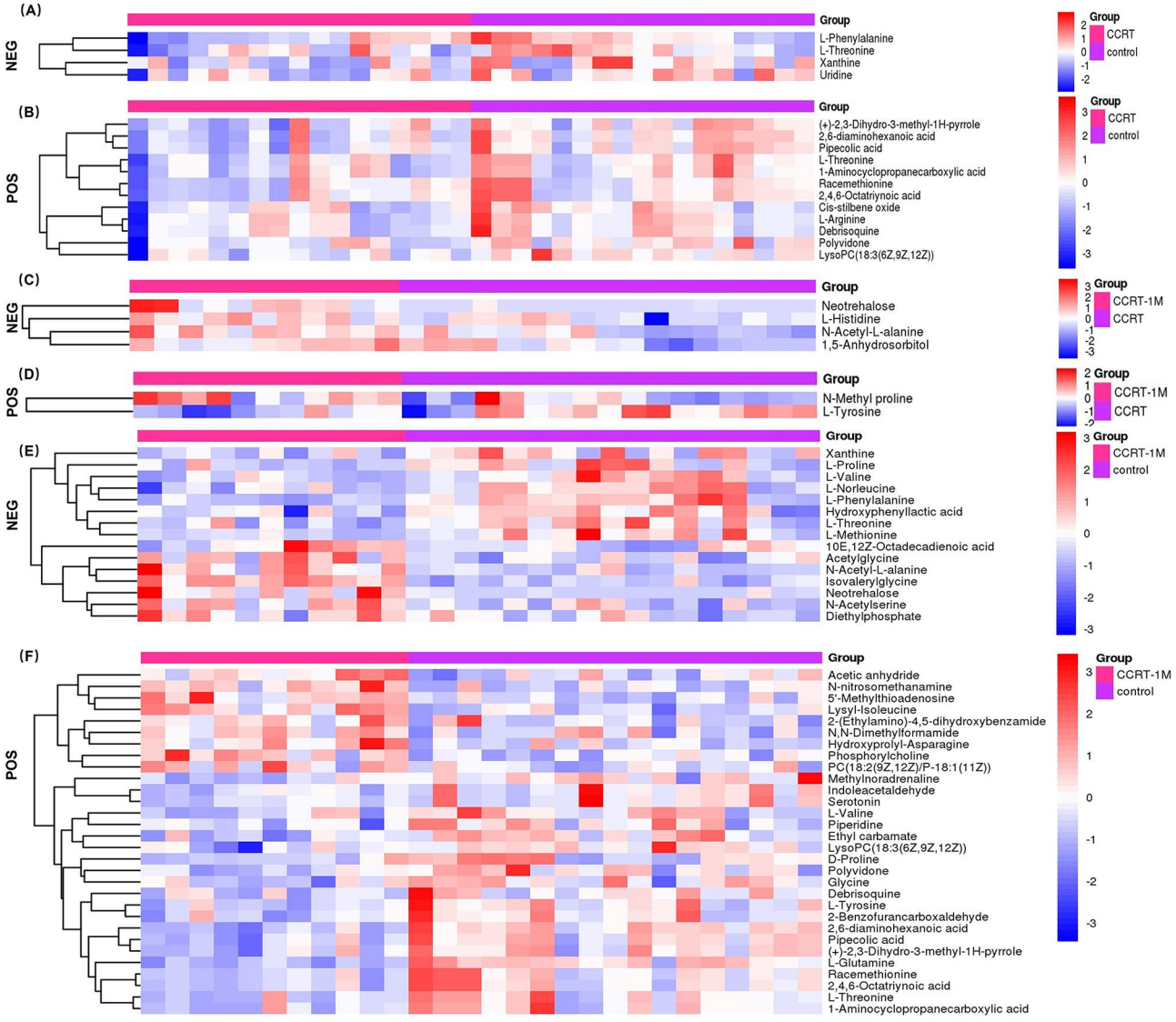

Fig. 3 Heatmap of hierarchical clustering analysis. **A** NEG Mode: Heatmap of hierarchical clustering for CCRT vs. Control group. **B** POS Mode: Heatmap of hierarchical clustering for CCRT vs. Control group. **C** NEG Mode: Heatmap of hierarchical clustering for CCRT-1 M vs. CCRT group. **D** POS Mode: Heatmap of hierarchical clustering for CCRT-1 M vs. CCRT group. **E** NEG Mode: Heatmap of hierarchical clustering for CCRT-1 M vs. Control group. **F** POS Mode: Heatmap of hierarchical clustering for CCRT-1 M vs. Control group. In each heatmap, the horizontal axis represents different sample groups, while the vertical axis displays all metabolites. The color blocks indicate relative metabolite expression levels, with red signifying high expression and blue indicating low expression

Furthermore, phenylketonuria, a genetic metabolic disorder, disrupts proper phenylalanine metabolism, and lysine can be converted into phenylalanine in the body, necessitating dietary restrictions on lysine intake for patients with phenylketonuria. Phenylalanine also serves as a precursor in tyrosine biosynthesis. Our pathway analysis indicates that the dysregulation of metabolic pathways, especially in phenylalanine, tyrosine, and tryptophan biosynthesis, is characteristic of ESCC and closely associated with CCRT susceptibility.

A recent study identified phenylalanine, 4-hydroxyphenylalanine, 3,4-dihydroxyphenylalanine, 3,4-dihydroxyphenylacetic acid, and tyrosine as diagnostic biomarkers in ESCC and metastatic ESCC [17]. Expression levels of tyrosine and its precursor, phenylalanine, were notably higher in patients with ESCC compared to healthy controls, supporting our findings that after CCRT treatment, lysine, phenylalanine, and tyrosine levels demonstrated a downward trend. This decline aligns with patient efficacy assessments based on CT and RECIST 1.1 criteria, indicating significant CCRT efficacy in patients with ESCC.

A prior clinical study reported that in patients with ESCC and lung cancer post-surgery, glutamine, total

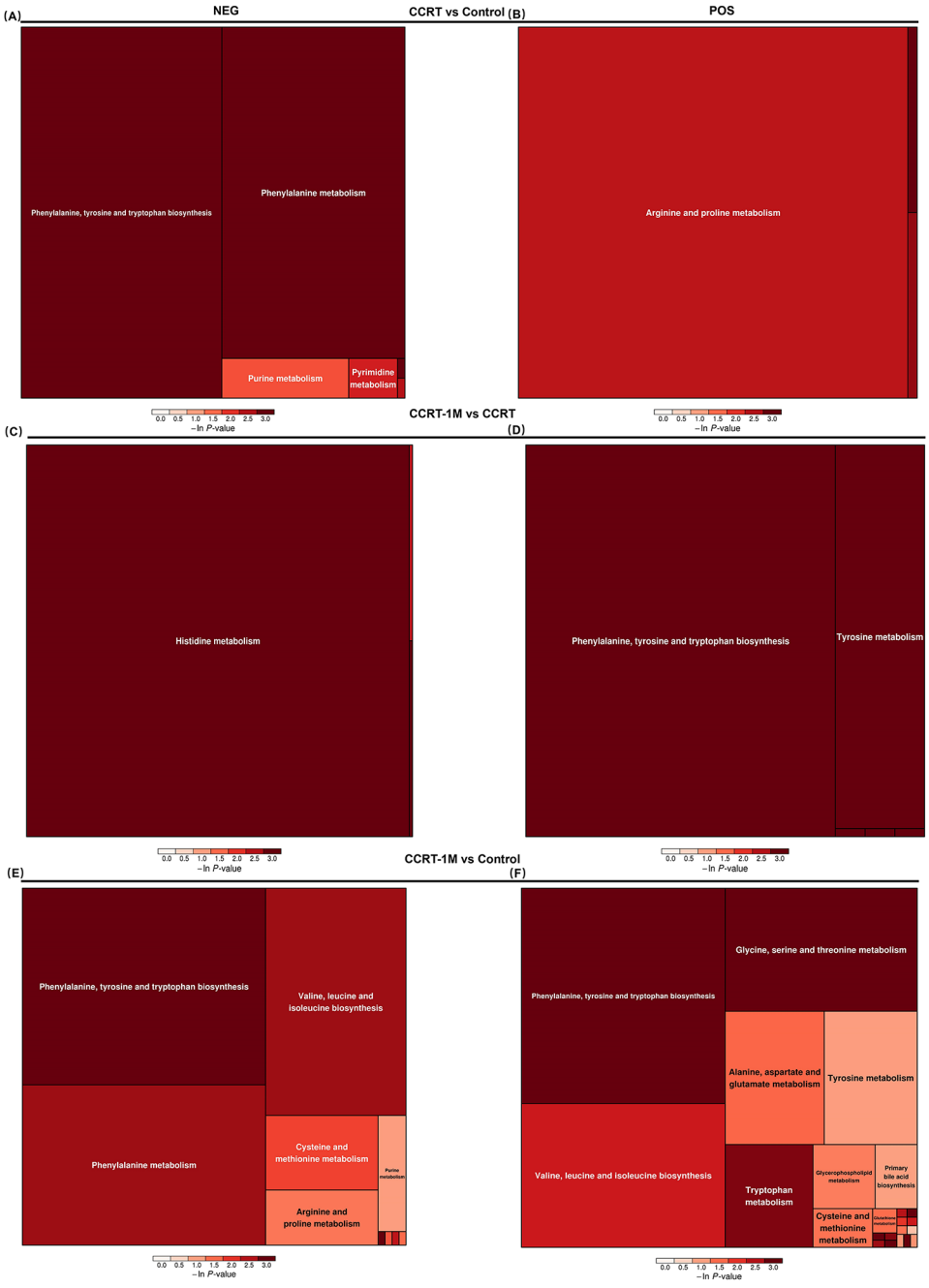

Fig. 4 Pathway analysis of differential metabolites. **A** NEG Mode: Pathway analysis for CCRT vs. Control group. **B** POS Mode: Pathway analysis for CCRT vs. Control group. **C** NEG Mode: Pathway analysis for CCRT-1 M vs. CCRT group. **D** POS Mode: Pathway analysis for CCRT-1 M vs. CCRT group. **E** NEG Mode: Pathway analysis for CCRT-1 M vs. Control group. **F** POS Mode: Pathway analysis for CCRT-1 M vs. Control group. In the rectangular tree diagram, each square represents a metabolic pathway. The square's size reflects the influence factor of the pathway in topological analysis—the larger the square, the higher the influence factor. The color of each square represents the P value of the enrichment analysis (shown as the negative natural logarithm, -ln(p)), with darker colors indicating smaller P values and thus a higher degree of enrichment. Pathways with significant enrichment are typically highlighted as dark, large squares

tryptophan, alanine, glycine, and arginine concentrations dropped significantly, while phenylalanine, lysine, valine, and leucine concentrations showed minimal change or were unaffected [18]. Contrastingly, our study observed a marked decline in phenylalanine, lysine, and valine levels following CCRT. In the CCRT-1 M vs. Control and CCRT-1 M vs. CCRT groups, phenylalanine and lysine levels differed significantly ($P < 0.05$), and valine expression in the CCRT-1 M vs. Control group was also significantly distinct ($P < 0.05$). Combined with AUC analysis

Table 3 ROC curves of differential metabolites

Group		Name	AUC	95 CI%
CCRT vs. Control	NEG	L-Phenylalanine	0.6816609	0.496148214725175-0.867173584582783
		L-Threonine	0.674740484	0.488670796023486-0.860810172834646
		Uridine	0.698961938	0.514334611635078-0.883589263797448
		Xanthine	0.69550173	0.511217259148713-0.879786201058899
	POS	(+)-2,3-Dihydro-3-methyl-1 H-pyrrole	0.771626298	0.60103128698105-0.94222130817466
		1-Aminocyclopropanecarboxylic acid	0.702422145	0.522031725065034-0.882812565592405
		2,4,6-Octatriynoic acid	0.705882353	0.527108668110538-0.884656037771815
		2,6-diaminohexanoic acid	0.809688581	0.651182483925103-0.968194678704655
		Cis-stilbene oxide	0.719723183	0.53984342351565-0.899602943266357
		Debrisoquine	0.674740484	0.491315955034892-0.85816501382324
		L-Arginine	0.660899654	0.474613802888728-0.847185505069749
		L-Threonine	0.716262976	0.539559473980909-0.892966477576184
		LysoPC(183(6Z,9Z,12Z))	0.757785467	0.590663318719525-0.92490761553653
		Pipecolic acid	0.78200692	0.619701584738571-0.944312256091879
		Polyvidone	0.740484429	0.557892402367888-0.9230764557636
		Racemethionine	0.692041522	0.512161762615996-0.871921282366703
CCRT-1 M vs. CCRT	NEG	1,5-Anhydrosorbitol	0.748663102	0.561780520160678-0.935545683047878
		L-Histidine	0.754010695	0.563309558984497-0.944711831389834
		N-Acetyl-L-alanine	0.85026738	0.700494095362645-1
		Neotrehalose	0.807486631	0.602046556106007-1
	POS	N-Methyl proline	0.780748663	0.59166734444351-0.969829981759698
		L-Tyrosine	0.79144385	0.614875572873293-0.968012127661467
CCRT-1 M vs. Control	NEG	10E,12Z-Octadecadienoic acid	0.695187166	0.47795407374197-0.912420257808833
		Acetylglycine	0.812834225	0.612600123204799-1
		Diethylphosphate	0.754010695	0.545887793144531-0.962133597229801
		Isovalerylglycine	0.983957219	0.948568983635636-1
		N-Acetyl-L-alanine	0.86631016	0.69142192387939-1
		N-Acetylserine	0.812834225	0.649089192206185-0.976579256991676
		Neotrehalose	0.786096257	0.567395292940581-1
		Hydroxyphenyllactic acid	0.786096257	0.608535317765955-0.963657195603029
		L-Methionine	0.79144385	0.618863531432466-0.964024169102293
		L-Norleucine	0.79144385	0.621105969586718-0.961781730948041
		L-Phenylalanine	0.903743316	0.794405391830982-1
		L-Proline	0.727272727	0.530818665733975-0.923726788811479
		L-Threonine	0.786096257	0.60370570060535-0.968486812763634
		L-Valine	0.823529412	0.664843827512815-0.982214996016597
		Xanthine	0.759358289	0.577888559920093-0.940828017620014
	POS	2-(Ethylamino)-4,5-dihydroxybenzamide	0.770053476	0.591082903727427-0.949024048144231
		5′-Methylthioadenosine	0.877005348	0.745479141490176-1
		Acetic anhydride	0.770053476	0.590898856471105-0.949208095400553
		Hydroxyprolyl-Asparagine	0.860962567	0.722916215460533-0.999008918229307
		Lysyl-Isoleucine	0.877005348	0.735442704740673-1
		N-nitrosomethanamine	0.871657754	0.72703389139055-1
		N, N-Dimethylformamide	0.77540107	0.596162158220414-0.954639980817019
		PC(182(9Z,12Z)P-181(11Z))	0.727272727	0.508973972538174-0.945571482007281
		Phosphorylcholine	0.86631016	0.699697075578015-1
		(+)-2,3-Dihydro-3-methyl-1 H-pyrrole	0.818181818	0.646646990795147-0.989716645568489
		1-Aminocyclopropanecarboxylic acid	0.79144385	0.606607800245986-0.976279900288773
		2-Benzofurancarboxaldehyde	0.77540107	0.591443742249532-0.959358396787901
		2,4,6-Octatriynoic acid	0.823529412	0.664835174374097-0.982223649155314
		2,6-diaminohexanoic acid	0.946524064	0.868476876269516-1
		D-Proline	0.700534759	0.491779423641005-0.909290095075573
		Debrisoquine	0.732620321	0.536607108538598-0.928633533172632

Table 3 (continued)

Group	Name	AUC	95 CI%
	Ethyl carbamate	0.79144385	0.617958841537061--0.964928858997698
	Glycine	0.759358289	0.570844280805377-0.94787229673473
	Indoleacetaldehyde	0.705882353	0.507072884567063-0.90469182131529
	L-Glutamine	0.957219251	0.87181283009042-1
	L-Threonine	0.834224599	0.669351343360094-0.999097854500868
	L-Tyrosine	0.79144385	0.619038667185608-0.963849033349151
	L-Valine	0.737967914	0.5477209579405-0.928214870936506
	LysoPC(183(6Z,9Z,12Z))	0.770053476	0.582921237873546-0.957185713998111
	Methylnoradrenaline	0.812834225	0.64910596506486-0.976562484133001
	Pipecolic acid	0.85026738	0.696441525994008-1
	Piperidine	0.695187166	0.495296248573104-0.895078082977698
	Polyvidone	0.754010695	0.568544246535535-0.939477143838797
	Racemethionine	0.818181818	0.653892600066986-0.98247103629665
	Serotonin	0.721925134	0.528599431687874-0.915250835691805

and comparative metabolomics results, this suggests that L-phenylalanine and lysine could serve as potential serum biomarkers for predicting CCRT efficacy, highlighting the link between CCRT treatment and ESCC progression.

Metabolites, as end-products of biochemical processes, closely reflect the physiological and pathological state of individuals [19]. Changes in metabolite levels in biological fluids (serum, plasma, urine) have been associated with prognosis, recurrence, and treatment response in patients with cancer [20–22]. A recent plasma metabolomic analysis of patients with ESCC exhibiting complete and incomplete pathological responses identified citrate cycling, glyoxylate, and dicarboxylate pathways as linked to chemoradiotherapy susceptibility in ESCC [23]. Serum metabolomic analysis in our study showed comparable findings, indicating that patients with ESCC exhibit reduced glucose metabolism (e.g., glycolysis, TCA, gluconeogenesis) after CCRT.

Additionally, a metabolomic study of serum samples from 137 patients with esophageal cancer highlighted glycine, serine, and threonine metabolism, as well as glycine, as potentially overlapping pathways and metabolites associated with disease progression and treatment efficacy [24]. Our serum metabolomics analysis in the CCRT-1 M vs. Control comparison revealed that differential metabolites impacted phenylalanine, tyrosine, and tryptophan biosynthesis, as well as glycine, serine, and threonine metabolism. These findings suggest that metabolic regulation one month after CCRT is associated with ESCC progression.

One of the root causes for the decrease of metabolites in patients with ESCC after CCRT and chemotherapy may be the effect of radiotherapy and chemotherapy on cell metabolism. Radiotherapy and chemotherapy may affect normal cells and cancer cells, thereby interfering with normal metabolic processes of cells, including protein synthesis and catabolism. L-phenylalanine is one of the important amino acids in protein synthesis. The disorder of cellular metabolism may lead to a decrease of its uptake and utilization, thus reducing its content in the body. Lysine is another essential amino acid, its synthesis and uptake in cells may be also inhibited, while its catabolism may increase, resulting in a decreased content in the patients after treatment with radiotherapy and chemotherapy.

In addition, radiotherapy and chemotherapy may cause systemic inflammatory reactions in patients, which affects the nutrient metabolism of the body, resulting in increased consumption and reduced utilization efficiency of various nutrients including L-phenylalanine and lysine. Moreover, chemoradiotherapy may also cause oxidative stress in patients, which interferes with normal cellular physiological processes, such as amino acid metabolism and transport. Notably, the specific mechanism may vary based on the physical status of patients. Therefore, further study is also necessary to enlarge cohorts' size of ESCC cases for comparing the serum metabolites to support the clinical significance of serum metabolites according to the response to CCRT.

Glucose is fundamental to life, serving as both an energy source and a carbon source for growth. Type 2 diabetes mellitus (T2DM) and cancer are two significant global health challenges, yet findings regarding their relationship with esophageal cancer have been inconclusive. While three meta-analyses have suggested a positive association between T2DM and esophageal cancer, these results are potentially unreliable due to high heterogeneity and confounding factors in the included studies [25]. In contrast, a large-scale cohort study involving 4,501,578 Black and White U.S. veterans reported that men with T2DM exhibited a reduced risk of esophageal cancer [26]. Similarly, studies examining T2DM and esophageal cancer risk within Australian and Asian populations

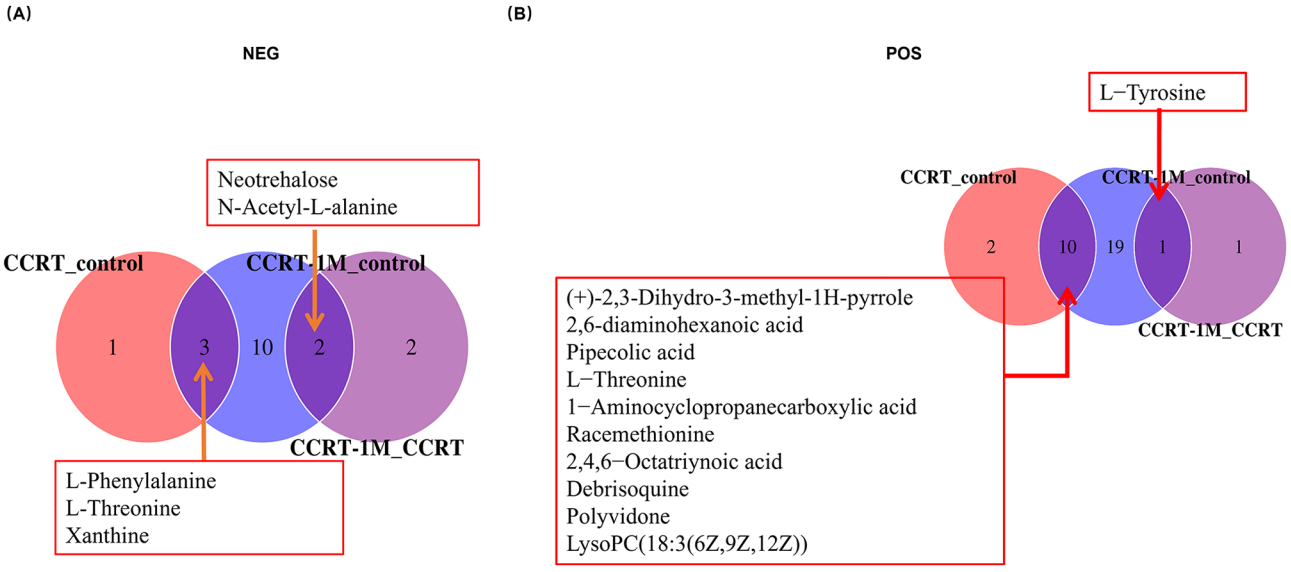

Fig. 5 Venn analysis for differential metabolites across comparison groups. **A** NEG Mode: Venn analysis illustrating shared and unique differential metabolites across CCRT vs. Control, CCRT-1 M vs. Control, and CCRT-1 M vs. CCRT comparisons. **B** POS Mode: Venn analysis for the same groups. Each circle represents a comparator group, with overlapping regions indicating the number of shared differential metabolites between groups, and non-overlapping sections showing metabolites unique to specific groups

found no link between diabetes diagnosis and esophageal cancer risk [27]. These conflicting findings underscore the need for further research into the role of T2DM in esophageal cancer development and mortality.

The body "burns" carbohydrates (sugars), proteins, and fats to generate the energy required for survival. Glucose plays a central role, providing both energy and carbon for growth. When glucose availability is restricted, cells rely on alternative nutrients to maintain metabolic functions. Cancer cells, in particular, demand high levels of energy to support rapid proliferation and survival, and they experience "hunger" without adequate nutrient sources. Despite this, esophageal tumors continue to grow, raising questions about their nutrient sources. Many amino acids, such as arginine, histidine, proline, threonine, phenylalanine, tyrosine, glycine, serine, and tryptophan [28, 29], are classified as glucogenic amino acids [30, 31]. These amino acids can be converted into pyruvate and other intermediates of the tricarboxylic acid cycle, thereby entering the gluconeogenesis pathway to produce glucose [32].

Research indicates that gluconeogenic amino acid levels in cancer are reduced due to accelerated hepatic gluconeogenesis aimed at supplying glucose to the tumor [33]. Additionally, factors like carbohydrate intolerance can influence amino acid concentrations. Findings show that metabolic pathways in cancer cells are repurposed to support tumor proliferation and regeneration, which increases cellular fuel demands [34].

Cancer cells exhibit adaptability under glucose scarcity. Recent studies have identified uridine as an essential nutrient source, highlighting its role as a precursor for RNA synthesis. Both cancer and immune cells can utilize uridine universally as a nutrient and energy source [35]. Targeting uridine metabolic pathways may therefore offer new avenues for treating cancer, managing metabolic disorders, and modulating immune responses. Further research has also shown that pancreatic cancer cells exploit uridine as an alternative nutrient source [36]. The ability of cancer cells to switch to alternative nutrients presents an opportunity: blocking this compensatory mechanism may pave the way for novel cancer treatments focused on "starving" cancer cells.

Conclusions

In conclusion, this study aims to optimize the therapeutic approach for patients with ESCC using CCRT and to identify potential biomarkers for prognosis monitoring. Findings confirm CCRT's substantial therapeutic impact on ESCC, with observed reductions in glucose metabolism pathways (e.g., glycolysis, TCA, gluconeogenesis) post-treatment. Additionally, L-phenylalanine and lysine are identified as potential serum biomarkers for predicting CCRT efficacy. Building on these findings, future

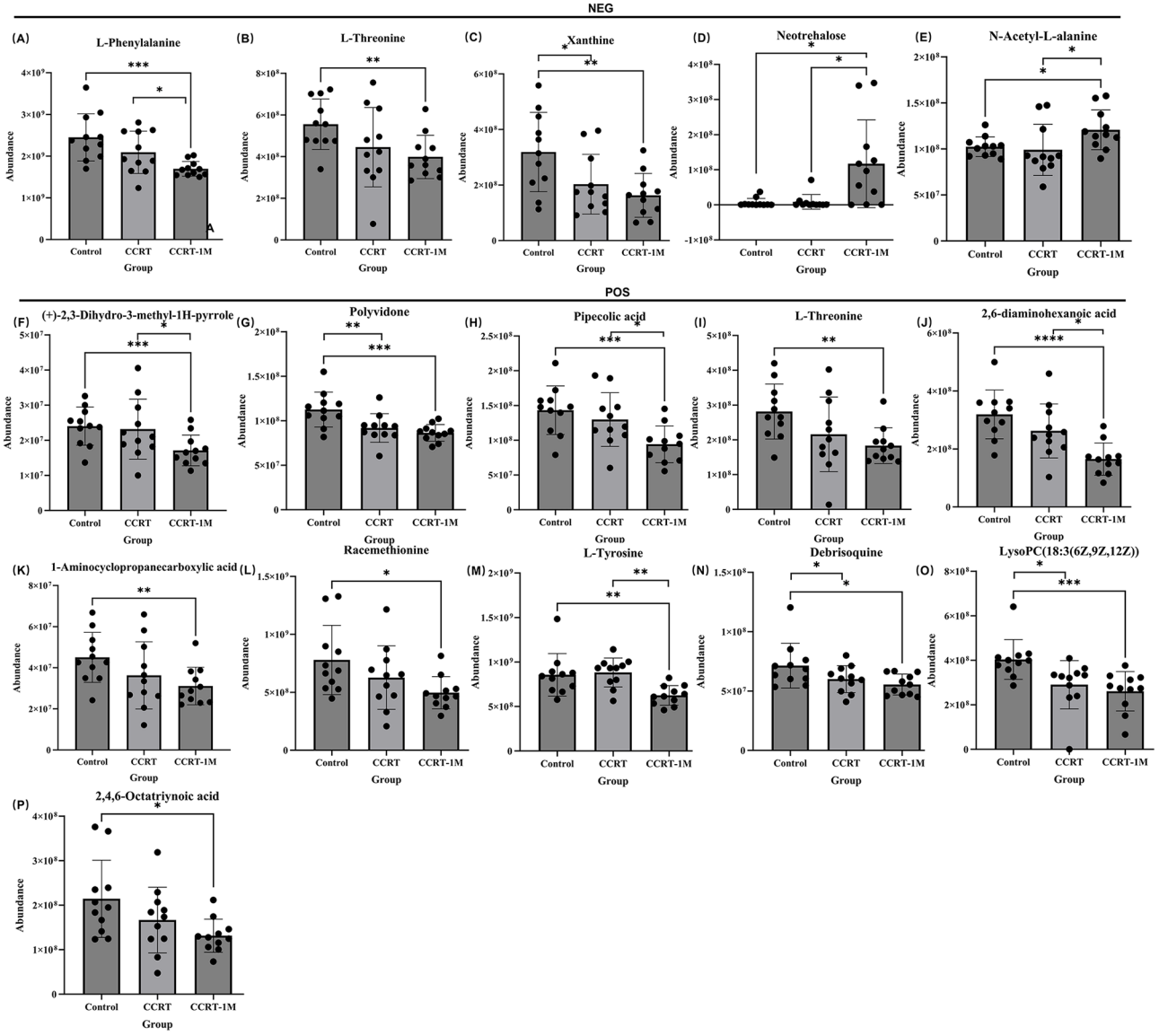

Fig. 6 Serum abundance of differential metabolites across Control, CCRT, and CCRT-1 M groups. NEG Mode: **A** Abundance of serum L-Phenylalanine in Control ($n=11$), CCRT ($n=11$), and CCRT-1 M ($n=11$) groups. **B** Abundance of serum L-Threonine across the three groups. **C** Abundance of serum Xanthine across the three groups. **D** Abundance of serum Neotrehalose across the three groups. **E** Abundance of serum N-Acetyl-L-alanine across the three groups. POS Mode: **F** Abundance of serum (+)-2,3-Dihydro-3-methyl-1 H-pyrrole across the three groups. **G** Abundance of serum Polyvidone across the three groups. **H** Abundance of serum Pipecolic acid across the three groups. **I** Abundance of serum L-Threonine across the three groups. **J** Abundance of serum 2,6-diaminohexanoic acid across the three groups. **K** Abundance of serum 1-Aminocyclopropanecarboxylic acid across the three groups. **L** Abundance of serum Racemethionine across the three groups. **M** Abundance of serum L-Tyrosine across the three groups. **N** Abundance of serum Debrisoquine across the three groups. **O** Abundance of serum LysoPC (18:3(6Z,9Z,12Z)) across the three groups. **P** Abundance of serum 2,4,6-Octatriynoic acid across the three groups. Statistical significance was determined using paired t-test analysis: $^{*}P<0.05$, $^{**}P<0.01$, $^{***}P<0.001$, and $^{****}P<0.0001$

work will expand the urine sample size for patients with ESCC to further the search for non-invasive predictive metabolic markers.

Abbreviations

CCRT	Concurrent chemoradiotherapy
ESCC	Esophageal squamous cell carcinoma
ICTP	Cross-linked carboxyterminal telopeptide of Type I collagen
QC	Quality control; PD: progressive disease
PR	Partial response
SD	Stable disease
SNCE	Stepped normalized collision energy
T2DM	Type 2 diabetes mellitus
TCA	Tricarboxylic acid

Acknowledgements
Not applicable.

Author contributions
JY: Data curation, Formal analysis, Validation, Investigation, Writing—original draft, Writing—review & editing. YYZ: Formal analysis, Validation, Investigation. YJZ: Formal analysis, Investigation. JY Z: Formal analysis, Investigation. YXW: Formal analysis, Investigation. YPL: Formal analysis, Writing—review &

editing. BZ: Formal analysis. JLX: Formal analysis. XLA: Formal analysis. XHQ: Formal analysis. YTY: Formal analysis, Methodology. LJZ: Formal analysis. XJZ: Formal analysis, Supervision, Resources. ZCF: Conceptualization, Supervision, Investigation, Data curation. KCL: Conceptualization, Resources, Data curation, Formal analysis, Supervision, Funding acquisition, Investigation, Methodology, Writing—original draft, Project administration, Writing—review & editing.

Funding
This work was supported by the National Natural Science Foundation of China (grant number 82273044), Science Fund for Distinguished Young Scholars of Fujian Province (grant number 2021D034), the Science Fund from the Health Commission of Fujian (grant number 2023GGB04), and Nantong University Clinical Medicine Special Scientific Research Fund Project (grant number 2024LZ014).

Data availability
The datasets supporting the conclusions of this article are included within the article, the collected data are not publicly available to protect patients' privacy and comply with ethical requirements, and the materials will be available upon requested.

Declarations

Ethics approval and consent to participate
This study was carried out in accordance with the World Medical Association Declaration of Helsinki, and it was approved by the ethics committee of the 900 Hospital of the Joint Logistics Team (Dongfang Hospital, Xiamen University) (Approval No. 2022-049), and the informed consents were signed by patients involved in this study.

Consent for publication
Not applicable.

Competing interests
The authors declare no competing interests.

Author details
[1]Central Laboratory, Danyang People's Hospital of Jiangsu Province, Danyang, Jiangsu 212300, P.R. China
[2]Department of Radiotherapy, 900 Hospital of the Joint Logistics Team, (Dongfang Hospital, Xiamen University), Fuzhou, Fujian 350025, P.R. China
[3]Central Laboratory, School of Medicine, Xiang'an Hospital of Xiamen University, Xiamen University, Xiamen, Fujian 361102, P.R. China
[4]School of Medicine, Xiamen University, Xiamen, Fujian 361102, P.R. China
[5]School of Life Science, Xiamen University, Xiamen, Fujian 361102, P.R. China

Received: 2 December 2024 / Accepted: 5 March 2025
Published online: 11 March 2025

References

1. Zhu H, Ma X, Ye T, Wang H, Wang Z, Liu Q, Zhao K. Esophageal cancer in China: practice and research in the new era. Int J Cancer. 2023;152(9):1741–51.
2. Li Q, Liu T, Ding Z. Neoadjuvant immunotherapy for resectable esophageal cancer: A review. Front Immunol. 2022;13:1051841.
3. van Hagen P, Hulshof MCCM, van Lanschot JJB, Steyerberg EW, van Berge Henegouwen MI, Wijnhoven BPL, Richel DJ, Nieuwenhuijzen GAP, Hospers GAP, Bonenkamp JJ, et al. Preoperative chemoradiotherapy for esophageal or junctional cancer. N Engl J Med. 2012;366(22):2074–84.
4. Pavlova NN, Thompson CB. The emerging hallmarks of Cancer metabolism. Cell Metab. 2016;23(1):27–47.
5. Pavlova NN, Zhu J, Thompson CB. The hallmarks of cancer metabolism: still emerging. Cell Metab. 2022;34(3):355–77.
6. Chen T, Xie G, Wang X, Fan J, Qiu Y, Zheng X, Qi X, Cao Y, Su M, Wang X, et al. Serum and urine metabolite profiling reveals potential biomarkers of human hepatocellular carcinoma. Mol Cell Proteom. 2011;10(7):M110004945.
7. Nabeya Y, Shimada H, Okazumi S, Matsubara H, Gunji Y, Suzuki T, Ochiai T. Serum cross-linked carboxyterminal telopeptide of type I collagen (ICTP) as a prognostic tumor marker in patients with esophageal squamous cell carcinoma. Cancer. 2002;94(4):940–9.
8. Liu K, Jiang M, Lu Y, Chen H, Sun J, Wu S, Ku WY, Nakagawa H, Kita Y, Natsugoe S, et al. Sox2 cooperates with inflammation-mediated Stat3 activation in the malignant transformation of foregut basal progenitor cells. Cell Stem Cell. 2013;12(3):304–15.
9. Liu K, Zhao T, Wang J, Chen Y, Zhang R, Lan X, Que J. Etiology, cancer stem cells and potential diagnostic biomarkers for esophageal cancer. Cancer Lett. 2019;458:21–8.
10. Zhao H, Wei Y, Zhang J, Zhang K, Tian L, Liu Y, Zhang S, Zhou Y, Wang Z, Shi S, et al. HPV16 infection promotes the malignant transformation of the esophagus and progression of esophageal squamous cell carcinoma. J Med Virol. 2023;95(10):e29132.
11. Liu K, Xie F, Zhao T, Zhang R, Gao A, Chen Y, Li H, Zhang S, Xiao Z, Li J, et al. Targeting SOX2 protein with peptide aptamers for therapeutic gains against esophageal squamous cell carcinoma. Mol Ther. 2020;28(3):901–13.
12. Wang Z, Wang J, Zhao H, Zhao T, Chen Y, Jiang M, Zhang S, Wei Y, Zhang J, Zhou Y, et al. Targeting the SOX2/PARP1 complex to intervene in the growth of esophageal squamous cell carcinoma. Biomed Pharmacother. 2022;153:113309.
13. Chen Y, Zhang K, Zhang R, Wang Z, Yang L, Zhao T, Zhang S, Lin Y, Zhao H, Liu Y, et al. Targeting the SOX2/CDP protein complex with a peptide suppresses the malignant progression of esophageal squamous cell carcinoma. Cell Death Discov. 2023;9(1):399.
14. Lin Y, Li X, Zhao J, Liu P, Zhou Y, Liu Y, Lin D, Bu L, Wang Z, Zhao H, et al. Agaricus Blazei murrill and Enteromorpha prolifera-derived polysaccharides gain therapeutic effects on esophageal squamous cell carcinoma. J Funct Foods. 2024;117:106244.
15. Buck A, Prade VM, Kunzke T, Feuchtinger A, Kröll D, Feith M, Dislich B, Balluff B, Langer R, Walch A. Metabolic tumor constitution is superior to tumor regression grading for evaluating response to neoadjuvant therapy of esophageal adenocarcinoma patients. J Pathol. 2022;256(2):202–13.
16. Wiggins T, Kumar S, Markar SR, Antonowicz S, Hanna GB. Tyrosine, phenylalanine, and Tryptophan in gastroesophageal malignancy: a systematic review. Cancer Epidemiol Biomarkers Prev. 2015;24(1):32–8.
17. Cheng J, Liu Q, Jin H, Zeng D, Liao Y, Zhao Y, Gao X, Zheng G. Integrating transcriptome and metabolome variability to reveal pathogenesis of esophageal squamous cell carcinoma. Biochim Biophys Acta Mol Basis Dis. 2021;1867(1):165966.
18. Naini AB, Dickerson JW, Brown MM. Preoperative and postoperative levels of plasma protein and amino acid in esophageal and lung cancer patients. Cancer. 1988;62(2):355–60.
19. Mamas M, Dunn WB, Neyses L, Goodacre R. The role of metabolites and metabolomics in clinically applicable biomarkers of disease. Arch Toxicol. 2011;85(1):5–17.
20. Qiu Y, Cai G, Zhou B, Li D, Zhao A, Xie G, Li H, Cai S, Xie D, Huang C, et al. A distinct metabolic signature of human colorectal cancer with prognostic potential. Clin Cancer Res. 2014;20(8):2136–46.
21. Alberice JV, Amaral AFS, Armitage EG, Lorente JA, Algaba F, Carrilho E, Márquez M, García A, Malats N, Barbas C. Searching for urine biomarkers of bladder cancer recurrence using a liquid chromatography-mass spectrometry and capillary electrophoresis-mass spectrometry metabolomics approach. J Chromatogr A. 2013;1318:163–70.
22. Mock A, Zschäbitz S, Kirsten R, Scheffler M, Wolf B, Herold-Mende C, Kramer R, Busch E, Jenzer M, Jäger D, et al. Serum very long-chain fatty acid-containing lipids predict response to immune checkpoint inhibitors in urological cancers. Cancer Immunol Immunother. 2019;68(12):2005–14.
23. Zhang Y, Wang J, Dai N, Han P, Li J, Zhao J, Yuan W, Zhou J, Zhou F. Alteration of plasma metabolites associated with chemoradiosensitivity in esophageal squamous cell carcinoma via untargeted metabolomics approach. BMC Cancer. 2020;20(1):835.
24. Yang X-L, Wang P, Ye H, Jiang M, Su Y-B, Peng X-X, Li H, Zhang J-Y. Untargeted serum metabolomics reveals potential biomarkers and metabolic pathways associated with esophageal cancer. Front Oncol. 2022;12:938234.
25. Yuan S, Kar S, Carter P, Vithayathil M, Mason AM, Burgess S, Larsson SC. Is type 2 diabetes causally associated with Cancer risk?? Evidence from a Two-Sample Mendelian randomization study. Diabetes. 2020;69(7):1588–96.
26. Atchison EA, Gridley G, Carreon JD, Leitzmann MF, McGlynn KA. Risk of cancer in a large cohort of U.S. Veterans with diabetes. Int J Cancer. 2011;128(3):635–43.

27. Harding JL, Shaw JE, Peeters A, Cartensen B, Magliano DJ. Cancer risk among people with type 1 and type 2 diabetes: disentangling true associations, detection bias, and reverse causation. Diabetes Care. 2015;38(2):264–70.
28. Altman BJ, Dang CV. Normal and cancer cell metabolism: lymphocytes and lymphoma. FEBS J. 2012;279(15):2598–609.
29. Vettore L, Westbrook RL, Tennant DA. New aspects of amino acid metabolism in cancer. Br J Cancer. 2020;122(2):150–6.
30. Brosnan JT. Interorgan amino acid transport and its regulation. J Nutr. 2003;133(6 Suppl 1):S2068–72.
31. Lieu EL, Nguyen T, Rhyne S, Kim J. Amino acids in cancer. Exp Mol Med. 2020;52(1):15–30.
32. Taherizadeh M, Khoshnia M, Shams S, Hesari Z, Joshaghani H. Clinical significance of plasma levels of gluconeogenic amino acids in esophageal Cancer patients. Asian Pac J Cancer Prev. 2020;21(8):2463–8.
33. Wahren J, Felig P, Cerasi E, Luft R. Splanchnic and peripheral glucose and amino acid metabolism in diabetes mellitus. J Clin Invest. 1972;51(7):1870–8.
34. Grasmann G, Smolle E, Olschewski H, Leithner K. Gluconeogenesis in cancer cells - Repurposing of a starvation-induced metabolic pathway? Biochim Biophys Acta Rev Cancer. 2019;1872(1):24–36.
35. Skinner OS, Blanco-Fernández J, Goodman RP, Kawakami A, Shen H, Kemény LV, Joesch-Cohen L, Rees MG, Roth JA, Fisher DE, et al. Salvage of ribose from uridine or RNA supports Glycolysis in nutrient-limited conditions. Nat Metab. 2023;5(5):765–76.
36. Nwosu ZC, Ward MH, Sajjakulnukit P, Poudel P, Ragulan C, Kasperek S, Radyk M, Sutton D, Menjivar RE, Andren A, et al. Uridine-derived ribose fuels glucose-restricted pancreatic cancer. Nature. 2023;618(7963):151–8.

Publisher's note